JOURNAL OF Materials CHEMISTRY

Crystal structure of the end product of electrochemical lithium intercalation in $V_2(SO_4)_3$†

Gavin B. M. Vaughan,*[a] Joël Gaubicher,[b] Thierry Le Mercier,[b] Jacques Angenault,[b] Michel Quarton[b] and Yves Chabre[c]

[a]*ESRF, BP 220, 38043 Grenoble Cedex, France. E-mail: vaughan@esrf.fr*
[b]*Laboratoire de Cristallochimie du Solide, Université Pierre et Marie Curie-Paris VI, 4 place Jussieu, 75252 Paris, Cedex 05, France*
[c]*Laboratoire de Spectrométrie Physique, Université Joseph Fourier-Grenoble I, Saint Martin d'Hères, France*

Received 5th July 1999, Accepted 10th August 1999

The crystal structure of $Li_2V_2(SO_4)_3$ obtained by electrochemical intercalation of lithium into $V_2(SO_4)_3$ has been solved using high resolution synchrotron X-ray powder diffraction. Surprisingly, in light of its 'soft chemistry' synthesis, the structure of $Li_2V_2(SO_4)_3$ is derived from that of the starting material *via* rearrangement of strong V–O bonds, leading to a mixed corner sharing/edge sharing arrangement among the VO_6 octahedra and SO_4 tetrahedra. Results of *in situ* electrochemical Li intercalation/synchrotron powder diffraction studies, carried out in working batteries and with a time resolution of the order of minutes, indicate that the rearrangement is reversible, at least during the first cycle.

Introduction

Many compounds of general formula $A_xM_2(XO_4)_3$ crystallise with open frameworks consisting of mutually corner-sharing XO_4 tetrahedra and MO_6 octahedra. Some of these compounds, with A = Li, M = transition metal, and X = S, P or As, are considered as excellent candidates for positive electrodes in rocking chair batteries.[1]

Recently, some of us[2] have investigated the electrochemical behaviour of one such system, $Li_xV_2(SO_4)_3$. The unintercalated starting product, $V_2(SO_4)_3$, has the rhombohedral $Fe_2(SO_4)_3$ (Nasicon-type) structure,[3] which can crystallographically accommodate up to four Li atoms per formula unit.

However, electrochemical and *in situ* X-ray diffraction data taken on the first cycle indicate that a first order phase transition occurs after the intercalation of *ca.* one Li per formula unit. The reduction process leading to the formation of two V^{2+} ions and corresponding to the intercalation of two Li per formula unit leads to the final product, nominally $Li_2V_2(SO_4)_3$. This material gave a diffraction pattern noticeably different from that of $Li_xV_2(SO_4)_3$ ($x \leqslant 1$); its structure could not be solved from the laboratory X-ray data. A sample was thus studied at the High Resolution Powder Diffraction Beamline (BM16) at the ESRF.

Experimental

A sample of $Li_2V_2(SO_4)_3$ was prepared by chemical lithium intercalation in $V_2(SO_4)_3$ using the *n*-butylithium technique. The sample was mounted under an inert atmosphere into a 0.5 mm borosilicate capillary. X-Ray diffraction confirmed that the chemically and electrochemically prepared $Li_2V_2(SO_4)_3$ samples present the same structure.

Powder diffraction data were taken at ESRF beamline BM16 over an angular range of 3–50° at a calibrated wavelength of 0.518098 Å. Data were collected by continuously scanning a 9-channel Ge(111) analyser/scintillation counter detector system.[4] These data were then combined into 0.01° bins for data analysis. See http://www.rsc.org/suppdata/jm/1999/2809/ for crystallographic files in .cif format.

Magnetic susceptibility was measured in the temperature range 4–300 K with a MANICS DSM8 susceptometer. The applied field was $0 \leqslant H \leqslant 17$ kOe. Field studies did not show evidence of ferri–ferromagnetic impurities.

Results

The indexing of the diffraction pattern was rather poor owing to the presence of weak peaks from one or more unidentified impurity phases and substantial overlap of the sample broadened peaks. As no indexation with a convincing quality factor M_{20}[5] was found, the most promising indexations from various runs of TREOR[6] were fed into Fullprof[7] for intensity extraction *via* the LeBail method.[8] A centred monoclinic cell was clearly favoured by the results of these attempts.

A partial structure solution was performed using direct methods,[9] which revealed the vanadium atoms. The sulfur and oxygen atoms were added with the connectivity softly constrained and the structure was completed by refining against the diffractogram using Profil.[10] Further Rietveld refinement of the V–O–S frame was performed with GSAS.[11] The structure was refined in the space group *C*2/*c* in order to facilitate comparison with the Nasicon structure.[12] The refined lattice parameters were $a = 13.0582(5)$, $b = 8.6526(4)$, $c = 8.7247(4)$ Å and $\beta = 115.443(2)°$, $Z = 4$. Subsequent Fourier difference maps clearly indicated the presence of a Li atom near (0.74, 0.41, 0.07); this position was subsequently refined and produced a significant improvement in the fit. Refinement of the lithium occupancy (with the Li thermal factors held constant) did not improve the refinement and the Li occupancy was fixed at unity in the final refinement. No further peaks $> 0.2\ e^-\ Å^{-3}$ remained in the difference maps. Refinement of anisotropic thermal factors did not produce a significant improvement in the refinement, thermal motion was thus treated isotropically in the final refinement. Final *R*-factors

†Supplementary data available: X-ray powder diffraction files in .cif format. For direct electronic access see http://www.rsc.org/suppdata/jm/1999/2809/, otherwise available from BLDSC (No. SUP 57620, 115 pp.). or the RSC Library. See Instructions for Authors, 1999, Issue 1 (http://www.rsc.org/materials).

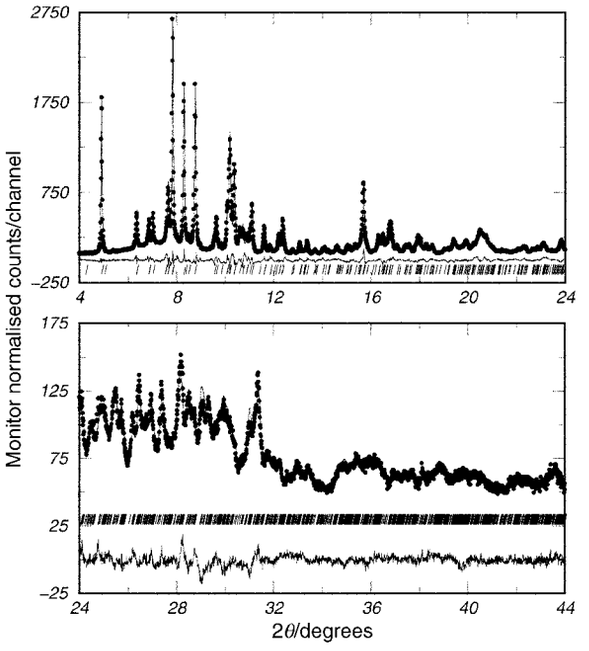

Fig. 1 Observed, calculated and difference patterns for $Li_2V_2(SO_4)_3$.

were $R_{wp}=6.5\%$, $R_p=5.0\%$, $R_{F^2}=4.2\%$, $R_e=6.9\%$. The observed and calculated diffraction patterns are shown in Fig. 1 and the final structural parameters are given in Table 1. Bond lengths and angles are presented in Table 2.

$Li_2V_2(SO_4)_3$ shows magnetic behaviour in agreement with the Curie–Weiss law above 50 K (Fig. 2). The molar Curie constant, C_m, and the paramagnetic Curie temperature, θ_p, as determined from the magnetic susceptibility. $\chi_M=C_M/(T-\theta_p)$ are $C_M=1.76(1)$ cm^3 K (mol V^{2+}), $\theta_p=-46(1)$ K. The corresponding value of the magnetic moment μ_{eff} (3.75) is close to the spin only value (3.87 μ_B) for a d^3 electronic configuration. The reciprocal molar magnetic susceptibility $1/\chi_M$ first decreases rapidly with lowering temperature before reaching a minimum near 25 K and thereafter rises. This behaviour is in accordance with an antiferromagnetic ordering of the d^3 paramagnetic centres consistent with the negative sign of the paramagnetic Curie temperature.

Discussion

Considering that the $V_2(SO_4)_3$ starting material has the rhombohedral $Fe_2(SO_4)_3$ structure,[13] which is a three dimensional network of corner sharing VO_6 octahedra and SO_4 tetrahedra, and the 'soft' electrochemical synthesis of $Li_2V_2(SO_4)_3$, the most striking feature of the $Li_2V_2(SO_4)_3$ structure (Fig. 3) is the observation of pairs of edge-sharing VO_6 octahedra not present in the starting material. Upon intercalation into $V_2(SO_4)_3$ one might expect a distorted structure such as that of monoclinic Nasicon,[12] rather than the observed bonding rearrangement. The relation between the

Table 1 Atomic positions and thermal factors of $Li_2V_2(SO_4)_3$

Atom	x	y	z	U_{iso}/Å
V	0.1232(2)	0.2500(4)	0.0145(3)	0.0036(6)
S(1)	0.3536(4)	0.1043(4)	0.3185(6)	0.0114(8)
S(2)	0	0.0592(5)	1/4	0.0114(8)
O(1)	0.1768(6)	0.4308(11)	0.1946(9)	0.0119(11)
O(2)	0.4717(7)	0.1341(8)	0.3809(9)	0.0119(11)
O(3)	0.3097(7)	0.1800(7)	0.4341(10)	0.0119(11)
O(4)	0.3008(7)	0.1648(8)	0.1530(9)	0.0119(11)
O(5)	0.4088(6)	0.4692(8)	0.1085(10)	0.0119(11)
O(6)	0.0583(7)	0.1529(8)	0.1719(9)	0.0119(11)
Li	0.744(2)	0.412(3)	0.068(3)	0.03

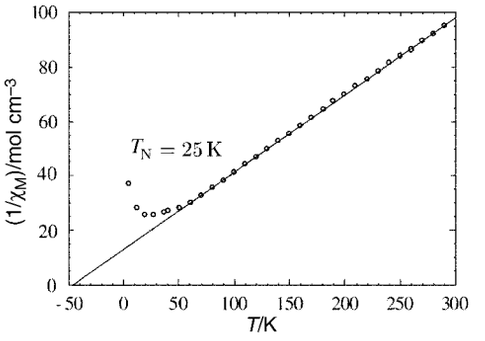

Fig. 2 Reciprocal molar magnetic susceptibility $1/\chi_M$ *vs.* T for $Li_2V_2(SO_4)_3$.

present structure and that of the starting product is shown in Fig. 4. Two corner connections between VO_6 and SO_4 polyhedra are broken and one of the SO_4 tetrahedra is rotated such that O(3), which no longer participates in a V–O bond, points toward a cavity. The two incomplete VO_6 octahedra are then brought together. The oxygen O(3) then coordinates to two lithium atoms at 1.90 and 2.10 Å.

As seen from the internal angles (Table 2), the SO_4 tetrahedra are only weakly distorted. However, the S(1)O_4 tetrahedron presents a large distribution of S–O bond lengths as each of the four oxygens has a different environment, O(1) coordinating in addition to V and Li, O(2) only to a V, O(3) to two Li, and O(4) to two V and more distantly to Li. The S(2)O_4 tetrahedra are elongated toward the O(5) atoms which are coordinated to V and Li. The O(6) atoms are coordinated only to a V.

In the geometrical description of the VO_6 octahedra, the main feature is the O(4)–V–O(4) angle, which is appreciably reduced from the ideal (Table 2). This correlates with the two long V–O(4) bond lengths and a shortening of the V–O(2) and V–O(6) bonds with respect to V–O(1) and V–O(5) perpendicular to this plane. These distances, resulting from V^{2+}–V^{2+} repulsion across the shared edge O(4)–O(4), are consistent with those observed in mixed corner-sharing/edge-sharing vanadium oxides such as V_2O_5,[14] V_4O_7 and V_5O_9.[15] It is also notable that the S–O(4) bond is the shortest of the S–O bonds, whereas the V–O(4) and Li–O(4) bonds are the longest of their types.

The lithium atoms show an irregular five-coordination (Table 2 and Fig. 5), with Li–O distances ranging from 1.88 to 2.32 Å. Each large cavity of the structural skeleton contains two Li atoms separated from each other by 3.04 Å and

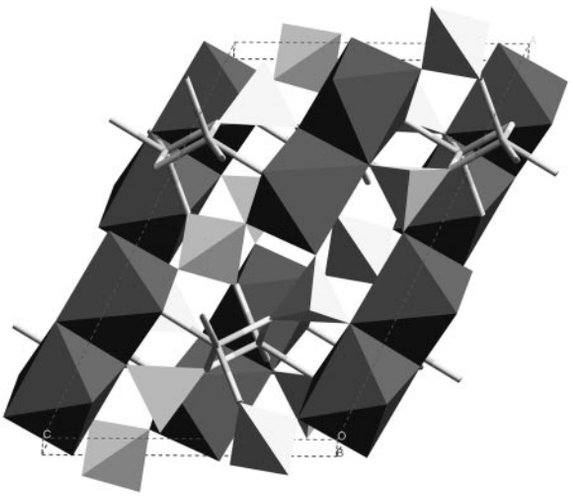

Fig. 3 Projection on (010) of the $Li_2V_2(SO_4)_3$ structure. VO_6 and SO_4 are shown in polyhedral representation; the coordination of the Li is shown as sticks.

Table 2 V–O, S–O, and Li–O bonds lengths (Å) and angles (°)

V–O(1)	2.113(7)	V–O(4)	2.229(7)	V–O(5)	2.130(7)	V–O(6)	2.076(7)
V–O(2)	2.074(8)	V–O(4)	2.215(7)				
O(1)–V–O(2)	89.5(3)	O(1)–V–O(6)	84.6(3)	O(2)–V–O(6)	90.3(3)	O(4)–V–O(5)	90.6(3)
O(1)–V–O(4)	84.6(3)	O(2)–V–O(4)	169.6(3)	O(4)–V–O(4)	79.1(3)	O(4)–V–O(6)	175.3(4)
O(1)–V–O(4)	98.3(3)	O(2)–V–O(4)	93.3(4)	O(4)–V–O(5)	85.0(3)	O(5)–V–O(6)	85.7(3)
O(1)–V–O(5)	164.7(4)	O(2)–V–O(5)	102.4(3)	O(4)–V–O(6)	97.6(3)		
S(1)–O(1)	1.544(9)	S(1)–O(3)	1.507(7)	S(2)–O(5)	1.512(8)	S(2)–O(6)	1.466(8)
S(1)–O(2)	1.421(8)	S(1)–O(4)	1.407(7)	S(2)–O(5)	1.512(8)	S(2)–O(6)	1.466(8)
O(1)–S(1)–O(2)	114.0(5)	O(2)–S(1)–O(3)	109.1(6)				
O(1)–S(1)–O(3)	108.2(4)	O(2)–S(1)–O(4)	107.4(5)				
O(1)–S(1)–O(4)	106.8(5)	O(3)–S(1)–O(4)	111.4(5)				
O(5)–S(2)–O(5)	118.0(7)	O(5)–S(2)–O(6)	106.2(3)				
O(5)–S(2)–O(6)	106.9(4)	O(5)–S(2)–O(6)	106.9(4)				
O(5)–S(2)–O(6)	106.2(3)	O(6)–S(2)–O(6)	112.9(6)				
Li–O(1)	1.88(3)	Li–O(3)	1.89(2)	Li–O(4)	2.32(3)	Li–O(5)	2.18(2)
Li–O(3)	2.13(2)						
O(1)–Li–O(3)	96.4(10)	O(1)–Li–O(5)	129.7(14)	O(3)–Li–O(5)	103.8(10)	O(3)–Li–O(5)	106.4(14)
O(1)–Li–O(3)	122.4(13)	O(3)–Li–O(3)	80.3(13)	O(3)–Li–O(4)	115.3(12)	O(4)–Li–O(5)	81.5(10)
O(1)–Li–O(4)	67.7(8)	O(3)–Li–O(4)	161.7(13)				

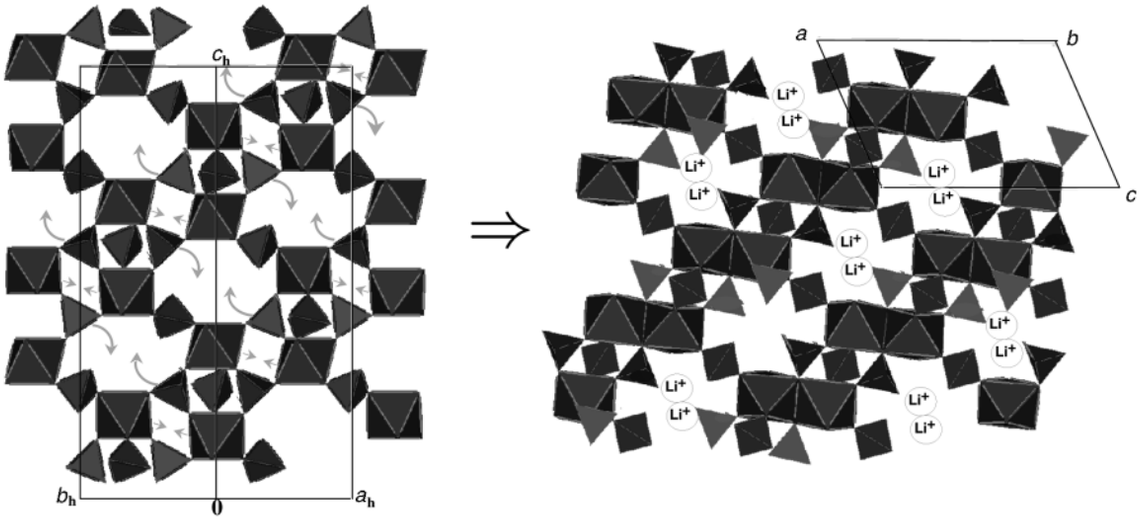

Fig. 4 The rearrangement mechanism for $V_2(SO_4)_3+2$ Li→$Li_2V_2(SO_4)_3$.

coordinated to four different types of oxygen atoms. The two LiO_5 polyhedra share edges consisting of O(3) atoms which do not participate in a V–O bond. This configuration, a consequence of localisation of Li in the cavities owing to its small ionic radius, has recently been described in another Nasicon type compound, $LiSn_2(PO_4)_3$.[16]

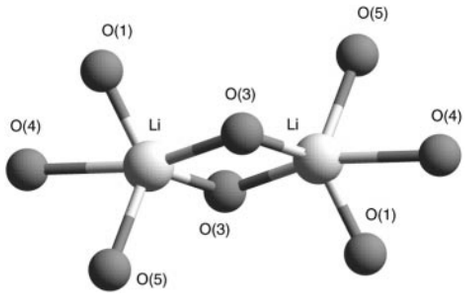

Fig. 5 Local environment of the lithium ions.

The low temperature antiferromagnetic behaviour of $Li_2V_2(SO_4)_3$ is in accord with that expected from a structure containing V_2O_{12} bioctahedra. Assuming that the local symmetry of the V^{2+} ions is O_h and that the magnetic exchange is the result of near-orthogonal (101°) V–O(4)–V super-exchange interactions, the magnetic behaviour would be ferromagnetic. Thus it seems that the direct interactions are predominant. Under such conditions, the rather long V^{2+}–V^{2+} distances (3.43 Å) are consistent with the low values of the Neél and paramagnetic temperatures (25 and −46 K, respectively) which indicate that the magnetic coupling is relatively weak.

Conclusion

The structure of $Li_2V_2(SO_4)_3$ has been solved by high resolution synchrotron X-ray powder diffraction. It is derived from the $V_2(SO_4)_3$ starting material not by simple Li intercalation, but by rearrangement of the structural skeleton polyhedra.

This unusual behaviour is most likely the consequence of the

small ionic radius of Li^+. During intercalation, Li^+ cations are bound with O^{2-} anions in the cavities of the Nasicon-type structure, weakening the V^{III}–O(3) bonds in VO_6 octahedra.

With a sufficient quantity of lithium [$Li_xV_2(SO_4)_3$ with $x > 1$], a majority of vanadium atoms are in the V^{II} state. This reduction of the vanadium leads to weakening of the V–O(3) bonds and an increase in vanadium–vanadium repulsion. Finally O(3) atoms are dissociated from the vanadium and the VO_6 octahedra coalesce in pairs in order to preserve their geometry. This mechanism appears to be particular to sulfates $Li_xM_2(SO_4)_3$, with strong S–O and weak M^{III}–O bonds. This behavior is not observed in homologous phosphates $Li_xM_2(PO_4)_3$, which show weaker P–O bonds and stronger M^{IV}–O bonds.

Interestingly, *in situ* diffraction studies carried out during electrochemical intercalation–deintercalation of $V_2(SO_4)_3$[17] indicate that this covalent rearrangement is also furthermore reversible, at least during the first cycle.

Acknowledgements

We thank the Powder Diffraction Beamline (BM16) at the ESRF for provision of synchrotron radiation beam time.

References

1 A. Manthiram and J. B. Goodenough, *J. Power Sources*, 1989, **26**, 403.
2 J. Gaubicher, Y. Chabre, J. Angenault, T. Le Mercier and M. Quarton, *Mol. Cryst. Liq. Cryst.*, 1998, **10**, 45.
3 P. A. Kokkoros, *Mineral. Petrogr. Mitt.*, 1965, **10**, 45.
4 J. L. Hodeau, P. Bordet, M. Anne, A. Prat, A. N. Fitch, E. Dooryhee, G. B. M. Vaughan and A. Freund, in *Proceedings of SPIE Conference on Crystal and Multilayer Optics*, San Diego, CA, 1998, vol. 3448.
5 P. M. de Wolff, *J. Appl. Crystallogr.*, 1968, **1**, 108.
6 P.-E.Werner, L. Eriksson and M. Westdahl, *J. Appl. Crystallogr.*, 1984, **18**, 167.
7 J. Rodriguez-Carvajal, Fullprof, Version 3.1c, Laboratoire Leon Brillouin, 1996.
8 A. L. Bail, H. Duroy and J. L. Fourquet, *Mater. Res. Bull.*, 1988, **23**, 447.
9 A. Altomare, G. Cascarano, C. Giacovazzo, A. Guagliardi, M. C. Burla, G. Polidori and M. Camalli, *J. Appl. Crystallogr.*, 1994, **27**, 435.
10 J. K. Cockcroft, Profil, Version 5.17, Birkbeck College, London, 1995.
11 A. C. Larson and R. B. Van Dreele, *GSAS—Generalized Structure Analysis System*, MS-H805, Los Alamos National Laboratory, 1990.
12 J. P. Boilot, G. Collin and P. Colomban, *Mater. Res. Bull.*, 1987, **22**, 669.
13 P. C. Cristides and P. J. Rentzeperis, *Z. Kristallogr.*, 1976, **144**, 341.
14 J. M. Cocciantelli, P. Gravereau, J. P. Doumerc, M. Pouchard and P. Hagenmuller, *J. Solid State Chem.*, 1991, **93**, 497.
15 H. Horiuchi, N. Morimoto and M. Tokonami, *J. Solid State Chem.*, 1976, **17**, 407.
16 E. Morin, J. Angenault, J. C. Coutirier, M. Quarton, H. He and J. Klinowski, *Eur. J. Solid State Inorg. Chem.*, 1997, **34**, 947.
17 J. Gaubicher, T. Le Mercier, C. Masquilier, J. Angenault, M. Quarton, Y. Chabre and G. Vaughan, in preparation.

Paper 9/05376J